JOC The Journal of Organic Chemistry

Article

pubs.acs.org/joc

Syntheses, Thermal Reactivities, and Computational Studies of Aryl-Fused Quinoxalenediynes: Effect of Extended Benzannelation on Bergman Cyclization Energetics

John D. Spence,* Andro C. Rios, Megan A. Frost, Claire M. McCutcheon, Christopher D. Cox, Sonia Chavez, Ramiro Fernandez, and Benjamin F. Gherman*

Department of Chemistry, California State University, Sacramento, Sacramento, California 95819, United States

Supporting Information

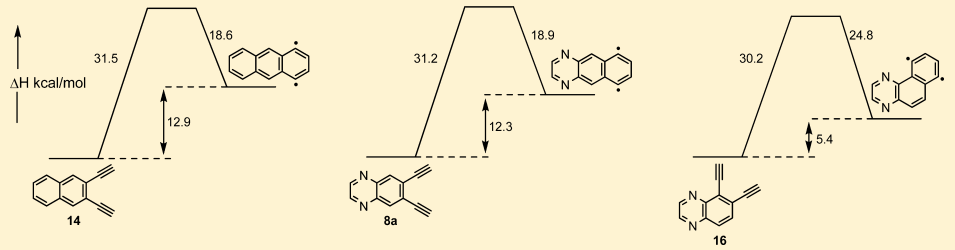

ABSTRACT: A series of [*b*]-fused 6,7-diethynylquinoxaline derivatives have been synthesized through an imine condensation strategy to examine the effect of extended benzannelation on the thermal reactivity of enediynes. Absorption and emission spectra of the highly conjugated quinoxalenediynes were red-shifted approximately 100−200 nm relative to those of 1,2-diethynylbenzene. Strong exotherms indicative of enediyne cyclization were observed by differential scanning calorimetry, while solution cyclizations in the presence of 1,4-cyclohexadiene confirmed C^1-C^6 Bergman cyclization. To provide further insight into Bergman cyclization energetics, computational studies were performed to compare changes in the cyclization enthalpy barrier, reaction enthalpy, and barrier of retro-Bergman ring-opening. Extension of benzannelation from 1,2-diethynylbenzene to either 2,3-diethynylnaphthalene or the 6,7-diethynylquinoxalines had a minimal effect on the cyclization barrier. In comparison, the enthalpies of cyclization were increased upon linearly extended benzannelation, which resulted in reduced barriers to retro-Bergman ring-opening. In addition, the orientation of extended benzannelation was found to have a significant effect on the cyclization endothermicity. In particular, 5,6-diethynylquinoxaline exhibited a 6.9 kcal/mol decrease in cyclization enthalpy compared to 6,7-diethynylquinoxaline due to increased aromatic stabilization energy in the respective angularly versus linearly fused azaacene cyclized products.

INTRODUCTION

Bergman cyclization[1] of enediynes provides an attractive method to generate highly reactive diradical intermediates en route to new aromatic rings. The parent cyclization of (*Z*)-hex-3-ene-1,5-diyne (**1**) to 1,4-didehydrobenzene (Figure 1) requires heating to 200 °C to overcome the relatively high activation energy due to electron repulsion of the filled in-plane alkyne π-orbitals.[2] The resulting 1,4-diradical intermediate, which lies in a substantial energy well upon gaining aromatic stabilization energy,[3] can undergo retro-Bergman ring-opening back to the enediyne (k_{-1}), radical chain polymerization processes, or irreversibly abstract hydrogen atoms from an appropriate donor to produce benzene (k_2). The initial resurgence in enediyne chemistry stemmed from the discovery of the naturally occurring enediyne antitumor antibiotics,[4] which employ Bergman cyclization to abstract hydrogen atoms from DNA, leading to double strand cleavage.[5] More recently, enediyne cyclizations have been utilized as a synthetic tool to prepare complex polycyclic aromatic hydrocarbons through Bergman[6] or related C^1-C^5 cyclizations initiated by external nucleophiles,[7] electrophiles,[8] radicals,[9] and transition metals.[10] Enediynes have also found material science applications as highly tunable fluorophores,[11] polymer initiators,[12] and precursors to highly conjugated aromatic polymers[13] and have facilitated the development of computational models to study diradical species.[14]

Incorporating the enediyne alkene within a benzene ring alters the reaction energetics for cyclization to the corresponding 1,4-diradical intermediate. Kinetic studies by Roth et al. on (*Z*)-hex-3-ene-1,5-diyne (**1**)[15] and 1,2-diethynylbenzene (**2**)[16] revealed a slightly lower activation enthalpy ($\Delta H^{\ddagger}$) with a significantly increased reaction enthalpy (ΔH_{rxn}) for cyclization upon benzannelation (Figure 1). Computational studies comparing the cyclization of **1** and **2** show the same general trends for the cyclization energetics,[14,17] though it is difficult to replicate the enthalpy of activation and the enthalpy of reaction with a single method. Increased endothermicity upon benzannelation has been attributed to a reduced gain in aromatic stabilization energy when transforming **2** to 1,4-didehydronaphthalene compared to the full aromaticity gain for the parent enediyne **1**.[18] The net

Received: September 14, 2012
Published: October 15, 2012

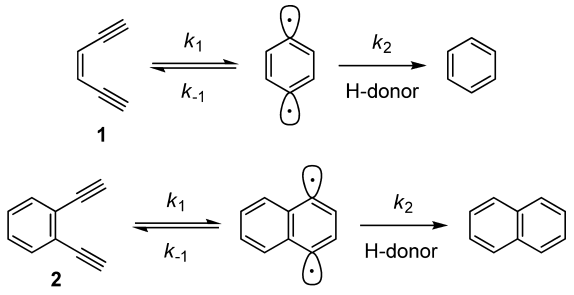

Compound	$\Delta H^{\ddagger}$	ΔH_{rxn}	$\Delta H^{\ddagger}_{retro}$
1	28.2	8.5	19.7
2	25.2	17.8	7.4

Figure 1. Bergman cyclization and experimental thermodynamic parameters (kcal/mol) for the cyclization of (*Z*)-hex-3-ene-1,5-diyne (**1**) (470 K) and 1,2-diethynylbenzene (**2**) (486 K).[15,16]

effect of benzannelation, therefore, reduces the barrier toward retro-Bergman ring-opening ($\Delta H^{\ddagger}_{retro}$) and makes hydrogen atom abstraction kinetically significant.[19] As a result, the overall rate of disappearance for **2** becomes dependent on the concentration of hydrogen atom donor,[20] while the rate of decay for simple alkyl derivatives of **1** is independent of the hydrogen atom donor concentration.[21] Addition of remote substituents to the aromatic ring of **2** was found to have a minor influence on the cyclization barrier through field effects as the developing radicals are orthogonal to the π-system of the benzene ring.[22] Appropriate *ortho* substituents, on the other hand, were found to decrease the cyclization barrier through steric assistance as the reactant has increased electron repulsion of the in-plane alkyne π-orbitals due to steric compression that is alleviated in the transition state.[23] For cyclic enediynes, the distance between the remote acetylenic carbons (c−d distance)[24] and ring strain[25] can further modulate cyclization barriers.

Annelation to the enediyne alkene has not been limited to a simple benzene ring as a variety of arenediynes (enediynes in which the alkene is contained within an aromatic ring) have been reported in the literature. Examples include enediynes fused to polycyclic aromatic hydrocarbons,[26] quinones and dihydroquinones,[27] and nitrogen heteroaromatics,[28] including porphyrin macrocycles.[29] Early interest in benzannelation was focused on monitoring the effect of the double bond character of the enediyne alkene on cyclization barriers.[27d] More recently, cyclic and phenylethynyl arenediynes have been employed for photochemical Bergman cyclization,[30] which requires locking the enediyne alkene in the *cis* configuration. Employing nitrogen heterocycles offers additional opportunities to improve delivery to biological targets and potential to modulate electronic properties of the enediyne through *N*-protonation and *N*-alkylation strategies.

In the present study, we investigate a series of [*b*]-fused 6,7-diethynylquinoxaline derivatives designed to readily alter the extent of benzannelation to the enediyne alkene. Increased benzannelation can offer improved DNA intercalation for biological applications and can provide synthetic access to a variety of highly conjugated azaacenes with tunable electronic properties.[31] With increased benzannelation, however, enediyne cyclization endothermicity is likely to increase while the retro-Bergman ring-opening barrier will further decrease compared to those of the parent enediyne **1**. Herein we present the synthesis, electronic properties, and thermal reactivity of a family of designed quinoxalenediynes. We also report our results from computational studies to evaluate the effects of extended benzannelation on Bergman cyclization barrier, reaction enthalpy for cyclization, and retro-Bergman ring-opening barrier for a series of benzannelated enediynes and related quinoxalenediynes.

RESULTS AND DISCUSSION

Syntheses. The general synthetic approach toward terminal [*b*]-fused 6,7-diethynylquinoxaline derivatives is outlined in Scheme 1. A key requirement in the design of our synthetic methodology was to develop a route that readily allowed us to alter the extent of benzannelation to the quinoxalenediyne core. This was accomplished through an imine condensation strategy employing aromatic 1,2-diones with appropriately functionalized diaminoarenediynes. For terminal quinoxalenediynes, Sonogashira coupling[32] of 1,2-diiodo-4,5-dinitrobenzene (**3**) with (trimethylsilyl)acetylene employing $Pd(PPh_3)_4$ and CuI in Et_3N produced nitroarenediyne **4** in 76% yield. The nitro groups were subsequently reduced with Zn in 10% AcOH/ethanol to generate our key diaminoarenediyne **5** in 99% yield. The silylated aryl-fused quinoxalenediynes **7a**−**7g** were then prepared from condensation of diamine **5** with glyoxal and aromatic 1,2-diones **6a**−**6g** under the conditions summarized in Table 1. Reaction

Scheme 1. Syntheses of [*b*]-Fused 6,7-Diethynylquinoxalines

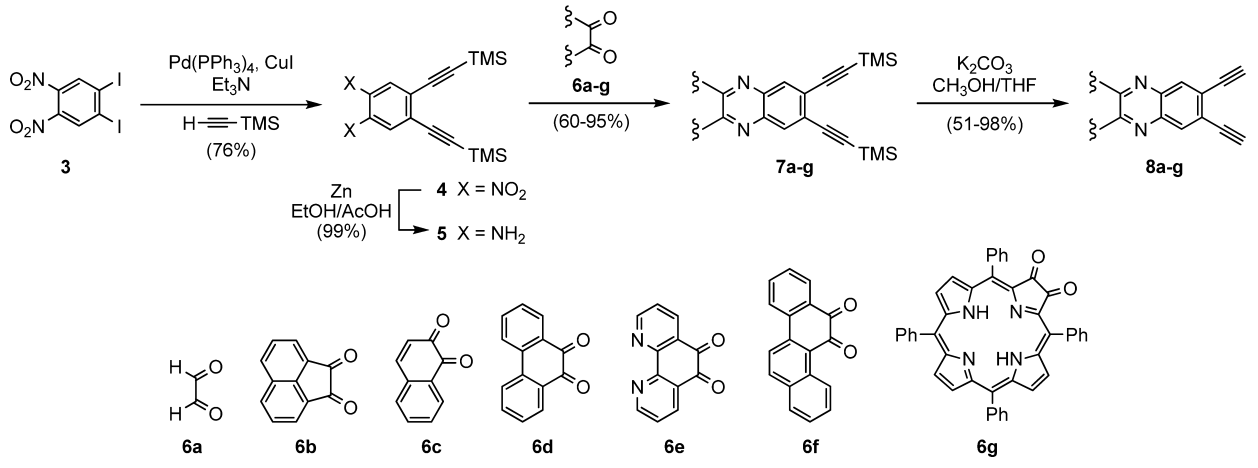

dx.doi.org/10.1021/jo302009c | *J. Org. Chem.* 2012, 77, 10329−10339

Table 1. Syntheses of Silylated and Terminal [*b*]-Fused 6,7-Diethynylquinoxalines

entry	1,2-dione	condensation[a] (% yield **7**)	desilylation[b] (% yield **8**)	product	
1	**6a**	70%[c]	98%	**8a**	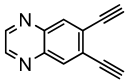
2	**6b**	89%	98%	**8b**	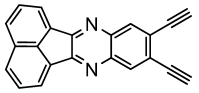
3	**6c**	60%[c]	93%	**8c**	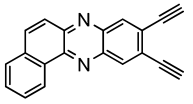
4	**6d**	95%	51%	**8d**	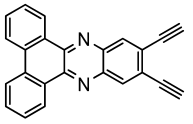
5	**6e**	89%	70%	**8e**	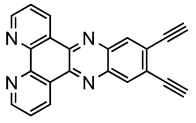
6	**6f**	85%	90%	**8f**	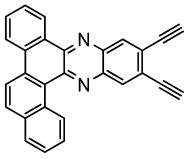
7	**6g**	90%[d]	90%	**8g**	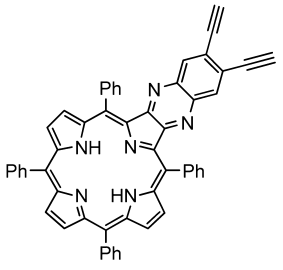

[a]Reaction conditions: **5** (1.0 equiv), **6** (1.0 equiv), 0.008 M C_6H_6, reflux, 12−72 h. [b]Reaction conditions: K_2CO_3, MeOH, THF, rt, 1 h. [c]Conducted at room temperature. [d]Conducted at room temperature in CH_2Cl_2.

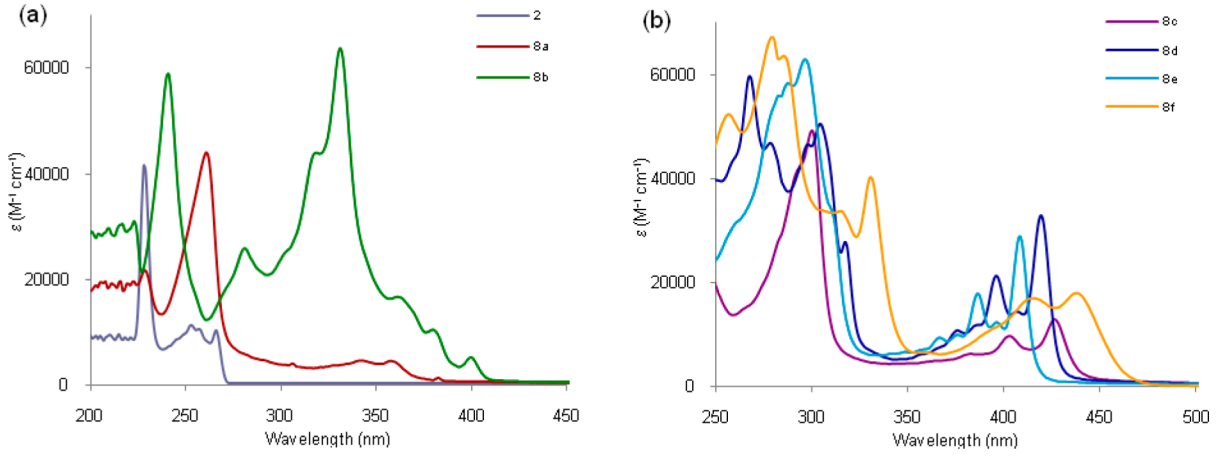

Figure 2. Electronic absorption spectra of (a) **2**, **8a**, and **8b** and (b) **8c**, **8d**, **8e**, and **8f** in CH_2Cl_2 at concentrations of (1.0−1.1) × 10^{-5} M.

with glyoxal (**6a**) (entry 1), 1,2-naphthoquinone (**6c**) (entry 3), and porphyrin-2,3-dione **6g** (entry 7) proceeded readily upon stirring at room temperature, while the remaining diones were less soluble and required heating to reflux in benzene to ensure reaction completion. For each substrate, products were isolated in good to excellent yields (60−95%) upon evaporation and purification by column chromatography.

Desilylation was accomplished by treatment with K_2CO_3 in CH_3OH/THF to yield [*b*]-fused 6,7-diethynylquinoxalines **8a**−**8g** upon filtration through a short plug of silica in 51−98% yields

dx.doi.org/10.1021/jo302009c | *J. Org. Chem.* 2012, 77, 10329−10339

(Table 1). Quinoxalenediynes **8a**–**8g** proved much less soluble than their silylated analogues **7a**–**7g**, and as a result, lower isolated yields were observed for certain substrates due to difficulties in purification. The structures of all [*b*]-fused 6,7-diethynylquinoxalines **8a**–**8g** were confirmed by ^{1}H NMR, ^{13}C NMR, and IR spectroscopies and high-resolution mass spectrometry.

Electronic Spectra. With increased conjugation, the absorbance spectra for the series of [*b*]-fused 6,7-diethynylquinoxaline derivatives gave bathochromic shifts compared to the spectrum of 1,2-diethynylbenzene (Figure 2, Table 2). The parent quinoxalenediyne **8a** gave two weak absorption bands at 358 and 342 nm, red-shifted by ∼90 nm compared to those of **2**, with a more intense higher energy band at 261 nm. Acenaphthoquinoxalenediyne **8b** gave an additional red shift with absorption bands out to 400 nm along with a more intense absorption at 331 nm. With added conjugation, naphthoquinoxalenediyne **8c**, phenanthroquinoxalenediyne **8d**, phenanthrolinoquinoxalenediyne **8e**, and chrysenoquinoxalenediyne **8f** all gave two strong absorptions extending into the visible region along with their most intense absorption near 300 nm. For naphthoquinoxalenediyne **8c**, increased benzannelation resulted in an additional 70 nm red shift compared to the spectrum of **8a**, with the longest wavelength absorbance extending out to 426 nm. **8d** and **8e** have increased molar extinction coefficients for visible absorptions with slightly smaller red shifts out to 419 and 408 nm, respectively. Finally, extended benzannelation in chrysenoquinoxalenediyne **8f** gave an absorption band at 440 nm, red-shifted by 80 nm compared to that of **8a** and over 170 nm compared to that of **2**. Extinction coefficients are in the 10000–30000 M^{-1} cm^{-1} range for visible absorptions, while those for the higher energy bands range from 40000 to 70000 M^{-1} cm^{-1}. For porphyrenediyne **8g**, the Soret band was observed at 421 nm with Q-bands at 531, 602, and 652 nm.

The electronic emission spectra for [*b*]-fused 6,7-diethynylquinoxalines **8b**–**8f** are shown in Figure 3 and summarized in Table 2. **8a** showed extremely weak fluorescence upon excitation at 261, 300, and 350 nm, and its emission spectrum is not shown in Figure 3. In comparison, excitation of compound **2** at 266 nm gave two emission bands at 309 and 318 nm with a relatively large Stokes shift. Compounds **8b**–**8e** all displayed similar excitation wavelength independent emission spectra upon excitation at 300, 350, and 400 nm in which the fluorescence intensity scaled according to absorbance at the excitation wavelength. Emission spectra for this series were characterized by two strong bands separated by approximately 20 nm and a weak shoulder at longer wavelengths. The highest energy emission band ranged from 405 to 439 nm, shifted by ∼100 nm compared to that of **2**, with much smaller Stokes shifts compared to those of **2**. Chrysenoquinoxalenediyne **8f**, on the other hand, exhibited low-intensity green fluorescence upon excitation at 400 nm with one broad emission band centered at 496 nm and a much larger Stokes shift. Porphyrenediyne **8g** gave two emission bands at 658 and 726 nm, slightly red-shifted compared to those of tetraphenylporphyrin.[33]

Table 2. Electronic Absorption and Emission Data

compd	λ_{max} (nm)[a] (ε, M^{-1} cm^{-1})	em λ_{max} (nm)	Stokes shift (cm^{-1})
2	266 (10400), 257 (10700)	309, 318	5230
8a	358 (4540), 342 (4630)	381	1690
8b	400 (5240), 380 (10480)	405, 427	310
8c	426 (15270), 403 (12090)	439, 459	700
8d	419 (32900), 396 (21300)	426, 449	390
8e	408 (31280), 397 (14610)	414, 437	360
8f	440 (18040), 417 (17060)	496	2570
8g	602 (11980), 531 (18810)	658, 726	1410

[a]Only the two lowest energy absorption maxima are listed.

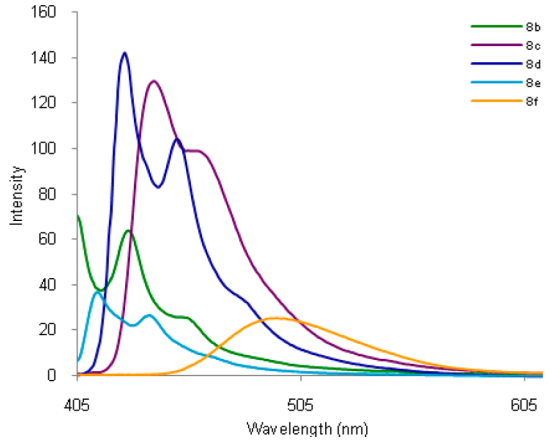

Figure 3. Electronic emission spectra of **8b**, **8c**, **8d**, **8e**, and **8f** in CH_2Cl_2 at concentrations of $(1.0–1.1) \times 10^{-5}$ M with an excitation wavelength of 400 nm.

Thermal Reactivity. The thermal reactivity of our series of [*b*]-fused 6,7-diethynylquinoxalines was initially probed by differential scanning calorimetry (DSC). While DSC provides a very crude estimate of relative enediyne reactivity, the observation of a well-defined exothermic peak is characteristic of enediyne cyclization and subsequent radical polymerization. Results of DSC measurements, recorded on neat solid samples of **8a**–**8g** with a 10 °C/min heating rate, are summarized in Table 3.

Table 3. DSC Data for [*b*]-Fused 6,7-Diethynylquinoxalines[a]

compd	T_{onset} (°C)	T_{max} (°C)	compd	T_{onset} (°C)	T_{max} (°C)
8a	178	189	**8e**	200	214
8b	194	209	**8f**	168	182
8c	173	197	**8g**	310	356
8d	164	174			

[a]Conditions: neat solid samples, 10 °C/min heating rate.

Under these conditions, 1,2-diethynylbenzene (**2**) gave an exotherm onset indicative of Bergman cyclization at 135 °C with a peak maximum at 165 °C. It should be noted, however, that 1,2-diethynylbenzene is a liquid sample whose reactivity is grossly overestimated by DSC as demonstrated by Alabugin.[23c] Quinoxalenediynes **8a**–**8g**, all of which are solids, uniformly gave higher onset and maximum temperatures compared to 1,2-diethynylbenzene. Onset temperatures ranged from 164 to 200 °C (30–70 °C higher than that of 1,2-diethynylbenzene), with temperature maxima ranging from 174–214 °C. This was expected with increased benzannelation, though there was no direct observable trend in onset temperature with respect to the extent of conjugation. Notably, phenanthroquinoxalenediyne **8d** gave the lowest onset temperature, while phenanthrolinoquinoxalenediyne **8e** and acenaphthoquinoxalenediyne **8b** gave the highest. Porphyrenediyne **8g** was an exception, with onset and maximum temperatures of 310 and 356 °C, respectively. The lack of correlation of the exotherm onset with the extent of conjugation, and large value for porphyrenediyne **8g**, is likely due to differences in crystal packing for the [*b*]-fused 6,7-

dx.doi.org/10.1021/jo302009c | J. Org. Chem. 2012, 77, 10329–10339

diethynylquinoxalines as no melting endotherms were observed by DSC. In fact, melting points for compounds **8a**–**8f** gave decomposition temperatures within 15 °C of the observed temperature maximum in DSC, indicating Bergman cyclization occurs prior to melting. Overall, these data support the conclusion of Alabugin that DSC, while a convenient measurement, is not a reliable method to compare trends in reaction energetics.

While DSC measurements provide an indication of thermal enediyne reactivity, samples run on neat liquids or solids give no information regarding product structure due to polymerization in the absence of a hydrogen atom donor. To determine the cyclization pathway, solution cyclizations were conducted on a preparative scale using representative examples. Thermal reactions were conducted on quinoxalenediyne **8a**, phenanthroquinoxalenediyne **8d**, and porphyrenediyne **8g** by heating solutions of enediyne in chlorobenzene containing 10% 1,4-cyclohexadiene at 180 °C for 24 h (Scheme 2). Each of the three

Scheme 2. Thermal Cyclization of [*b*]-Fused 6,7-Diethynylquinoxalines

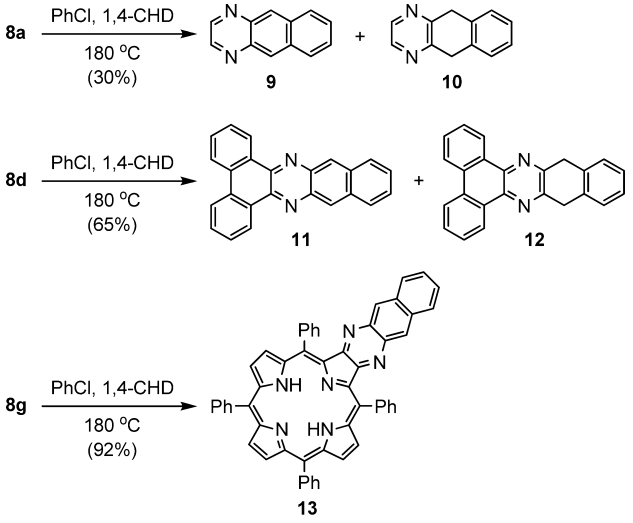

compounds underwent C^1–C^6 Bergman cyclization at this temperature; however, the benzoquinoxaline core in products **9** and **11** was further reduced by 1,4-cyclohexadiene to 5,10-dihydrobenzo[*g*]quinoxaline derivatives **10** and **12**. The presence of reduced products **10** and **12** was evident by a 4H singlet in the ^{1}H NMR spectra near 4 ppm and a methylene signal in the ^{13}C spectra. For quinoxalenediyne **8a**, an inseparable 3:1 mixture of **9** and **10** was obtained that, upon oxidation with DDQ, afforded pure benzo[*g*]quinoxaline (**9**) in 30% yield, with the remaining mass balance comprised of uncharacterized polymeric byproducts. In comparison, under similar conditions thermal cyclization of **2** gives naphthalene in 35% yield.[23c] For phenanthroquinoxalenediyne **8d**, 5,10-dihydrobenzoquinoxaline **12** was obtained as the major product in 65% yield with traces of benzoquinoxaline **11** that could not be separated as slow oxidation of **12** to **11** was observed. Porphyrenediyne **8g** gave a 92% yield of benzoquinoxalinoporphyrin **13**, with no observation of the reduced 5,10-dihydrobenzoquinoxaline derivative forming.[29e] The reactivity of **8g** at 180 °C provides additional evidence that crystal packing plays a significant role in DSC measurements on solid samples as DSC indicated a temperature onset above 300 °C.

Computational Analysis. To gain insight into the effect of extended benzannelation on Bergman cyclization energetics, we turned to a computational approach to measure activation barriers, reaction energies, and retro-Bergman ring-opening barriers. While computational studies of the Bergman cyclization involving diradical species can be challenging, unrestricted broken-symmetry density functional theory calculations can provide thermodynamic parameters in close agreement with experimental values. In addition to modeling the parent and benzannelated enediynes **1** and **2**, we have performed calculations on the extended derivative 2,3-diethynylnaphthalene (**14**) along with the three possible quinoxalenediyne isomers 2,3-diethynylquinoxaline (**15**), 5,6-diethynylquinoxaline (**16**), and 6,7-diethynylquinoxaline (**8a**) (Figure 4). Finally, **8c**, **8d**, and

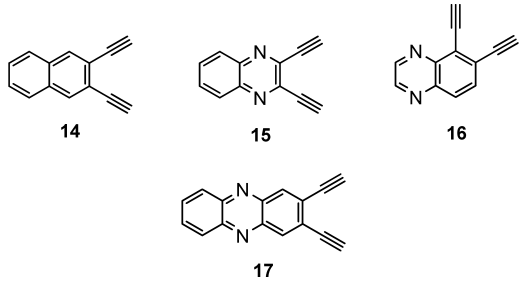

Figure 4. Structures of additional arenediynes examined with DFT calculations.

2,3-diethynylphenazine (**17**) have also been examined as representative examples of [*b*]-fused 6,7-diethynylquinoxaline derivatives. A detailed description of our computational methodology is provided in the Experimental Section. Computational results for **1** and **2**, compared to literature values, are given in Table 4, while thermodynamic parameters for all compounds studied, including retro-Bergman ring-opening barriers, are given in Table 5.

Table 4. Comparison of Theoretical (Gas Phase) and Experimental Thermodynamic Parameters (kcal/mol) for Compounds 1 and 2

compd	$\Delta H^{\ddagger}$ (470 K)	$\Delta G^{\ddagger}$ (470 K)	ΔH_{rxn} (298 K)	ref
1	29.59	32.97	0.88	this work
	32.3	36.5	10.2[a]	14[b]
	23.8		7.3	17[c]
	31.2[d]		3.3[d]	34[e]
	28.2	33.0	8.5	experiment[15]
2	30.37	33.77	9.18	this work
	32.8[f]	36.6[f]	17.8[f]	14[b]
	23.0		13.2	17[c]
	28.5[d]		13.4[d]	34[e]
	25.2[f]	35.6[f]	17.8	experiment[16]

[a]Value measured at 470 K. [b]B3LYP/6-311+G(3df,3pd)//B3LYP/6-31G(d,p) calculations. [c]BLYP/6-31G(d) calculations. [d]$\Delta E^{\ddagger}$ and ΔE values. [e]B3LYP/6-31G(d,p) calculations. [f]Value measured at 486 K.

We initially examined the effect of benzannelation on the enediyne core using our methodology on **1** and **2** (Table 4). While the computed cyclization $\Delta H^{\ddagger}$ values show a slight increase upon benzannelation, which is counter to the trend seen experimentally,[15,16] the results are consistent with other computational values reported in the literature.[14,17,34] Better agreement with experimental values is seen with $\Delta G^{\ddagger}$, which

dx.doi.org/10.1021/jo302009c | J. Org. Chem. 2012, 77, 10329–10339

Table 5. Computed Bergman Cyclization Thermodynamic Parameters (25 °C, Gas Phase, kcal/mol)

structure	compd	$\Delta H^{\ddagger}$	ΔH_{rxn}	$\Delta H^{\ddagger}_{retro}$
enediynes	**1**	30.03	0.88	29.15
	2	30.83	9.18	21.65
	14	31.49	12.89	18.60
quinoxalenediynes	**8a**	31.16	12.27	18.89
	15	30.49	10.82	19.67
	16	30.24	5.39	24.85
[*b*]-fused quinoxalenediynes	**8c**	31.29	13.15	18.14
	8d	31.27	12.89	18.38
	17	31.36	13.80	17.56

slightly increases according to both computation and experiment upon benzannelation. ΔH_{rxn}, on the other hand, markedly increases from 0.9 to 9.2 kcal/mol upon benzannelation. These trends continue upon extending benzannelation from **2** to 2,3-diethynylnaphthalene (**14**), wherein addition of a second benzene ring increases cyclization endothermicity an additional 3.7 kcal/mol (Table 5). These relative changes fit expectations based upon reduced aromatic stabilization energy gain for the diradical intermediate as the extent of benzannelation to the enediyne core is increased. As a result, the barrier for retro-Bergman ring-opening decreases by 7.5 kcal/mol upon initial benzannelation, while addition of a second benzene ring in **14** decreases the barrier toward retro-Bergman ring-opening an additional 3.1 kcal/mol (Table 5).

Considering the variety of density functional calculations used to study Bergman cyclization of **1** and **2**,[14,17,34,35] some notes should be made as to the reliability of the computational protocol applied herein. Activation enthalpies and activation free energies are as accurate or more accurate versus experimental data than values reported by Sherer et al.[14] and Prall et al.[17] On the other hand, computed enthalpies of reaction are lower than those from the other computational work and from experiment.[15,16] This difference must be viewed in light of the fact that most density functionals underestimate ΔH_{rxn} for Bergman cyclization.[35] However, the $\Delta\Delta H_{rxn}$ from **1** to **2** measured here is 8.3 kcal/mol versus 9.3 kcal/mol experimentally, for a difference of only 1.0 kcal/mol, which is less than that from alternative DFT results. Also, our singlet−triplet energy gap for the diradical product from **1** is in good agreement with experiment and previous computation (Table S1, Supporting Information).[14] Collectively, these comparisons suggest the challenge of selecting a single density functional capable of reproducing experimental thermodynamics across the entire Bergman cyclization reaction coordinate.[35] The present computational methodology, however, performs well for determining the activation enthalpies for cyclization and the change in reaction enthalpies for cyclization upon changing the extent of benzannelation.

We next examined the series of quinoxalenediynes, **8a** along with isomers **15** and **16**, to compare to 2,3-diethynylnaphthalene (**14**) (Table 5). For this series, the enthalpy barrier is slightly lowered compared to that of **14** as a result of the electron-withdrawing nitrogen atoms. This effect is stronger for **15**[14,36] and **16**, which places the nitrogen atoms closer to the enediyne core, while steric assistance between the *peri* nitrogen lone pair and in-plane alkyne π-orbital in **16** may further reduce the cyclization barrier. More dramatic changes are observed in the ΔH_{rxn} values for this series. While a slight decrease is observed for **8a** compared to **14** (0.6 kcal/mol), a larger decrease in reaction endothermicity is observed for **15** (2.0 kcal/mol) and **16** (7.5 kcal/mol). This results in larger $\Delta H^{\ddagger}$ values for retro-Bergman ring-opening for this series, with the retro barrier for **16** higher than even that of **2** and approaching the value calculated for **1**. The dramatic decrease in cyclization endothermicity for **16** suggests additional stabilization energy is available to the diradical intermediate derived from **16**. Upon inspection of the cyclized products, Bergman cyclization of **16** leads to an angularly fused polyphene containing a new aromatic sextet (Figure 5). In comparison, the extended annelation in **8a**, **14**, and

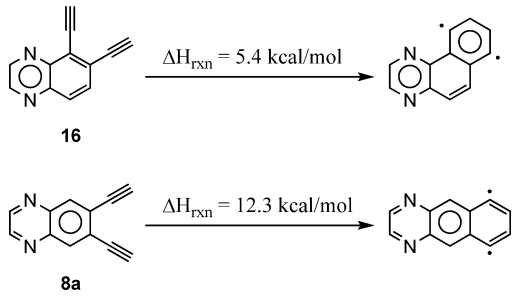

Figure 5. Application of Clar's rule to arenediyne cycloaromatization.

15 leads to linearly fused polyacenes in which only one six-membered ring possesses an aromatic sextet. In accordance with Clar's rule,[37] which states that a molecule with more explicit benzene sextets will be more aromatic, formation of a new aromatic sextet should increase the overall aromatic stabilization energy gain upon cyclization of **16**. The calculated 6.9 kcal/mol increase in stability for the diradical produced from **16** compared to the diradical produced from **8a** is in line with the experimentally measured total resonance energy difference of 7−12 kcal/mol between angularly fused phenanthrene and linearly fused anthracene.[38]

The decreased cyclization endothermicity of **16** indicates an influence of benzannelation on cyclization energetics not previously explored in detail. With appropriately oriented extended benzannelation, hydrogen atom abstraction may no longer be kinetically significant, as it is for simple benzannelation, due to an increased retro-Bergman ring-opening barrier. In this event, an irreversible Bergman cyclization would ensue, with formation of a new aromatic sextet driving the overall cyclization energetically. While the cyclization rates of 2,3-diethynylnaphthalene derivatives are reported to be slower than those of their corresponding diethynylbenzene counterparts,[20,39] the only report describing Bergman cyclization of an angularly fused 1,2-diethynylnaphthalene derivative is the seminal work on the photo-Bergman cyclization of *o*-dialkynylarenes by Funk and coworkers.[26] Curiously, in this report, the cyclic derivative of 1,2-diethynylnaphthalene undergoes photo-Bergman cyclization with 38% conversion, while the isomeric 2,3-diethynylnaphthalene analogue shows no reactivity under photochemical conditions. As the 1,2-diethynyl derivative produces a new aromatic sextet, while the 2,3-diethynyl derivative does not, application of Clar's rule on the stability of the resulting diradical intermediates may partially explain the difference in reactivity. While our computational results suggest an energetic effect which favors Bergman cyclization upon angularly extended benzannelation, additional work is necessary to fully understand this connection.

Finally, the [*b*]-fused quinoxalenediynes **8c**, **8d**, and **17** all gave similar activation enthalpies, reaction enthalpies, and retro-Bergman barriers compared to those of **8a** and **14**. With extended

linear benzannelation, **17** was the most endothermic, giving the smallest retro-Bergman barrier of all the systems studied. However, the enthalpy cost of adding a third fused ring upon extending linear benzannelation in **17** is significantly reduced compared to the initial cost of benzannelation in **2**. For **8c** and **8d**, angular benzannelation from **17** slightly reduces the reaction endothermicity. In this case, the angular benzannelated ring is further removed from the enediyne core, which does not lead to a new aromatic sextet upon cyclization as observed for **16**.

CONCLUSION

The above work describes the synthesis of a family of [*b*]-fused 6,7-diethynylquinoxalines designed to examine the influence of extended benzannelation on thermal enediyne reactivity. DSC analysis revealed exothermic peaks indicative of radical enediyne cyclization, while solution studies confirmed C^1-C^6 Bergman cyclization remains a viable reaction pathway thermally. Further reduction of the benzo[*g*]quinoxaline core in the cyclized product by 1,4-cyclohexadiene, and subsequent oxidation back to the fully aromatic derivative, reveals novel redox properties available to the azaacene cyclization products. According to our calculations, extending benzannelation from 1,2-diethynylbenzene in a linear fashion with respect to the enediyne core further increases C^1-C^6 cyclization endothermicity, while extending benzannelation in an angular orientation from the enediyne core reduces Bergman cyclization endothermicity. These trends may be summarized accordingly by Clar's rule, wherein arenediynes that produce new aromatic sextets lead to more favorable Bergman cyclization endothermicity due to increased aromatic stabilization energy gain. Furthermore, increased retro-Bergman ring-opening barriers should result in irreversible cyclizations with rates that are independent of the hydrogen atom donor concentration. Angular benzannelation further removed from the enediyne core, as in the present family of synthetic quinoxalenediyne derivatives, however, has a minor influence on the reaction energetics. We are in the process of examining solution cyclizations and computational analyses of cyclic and (phenylethynyl)quinoxalenediyne derivatives to determine what effect alkyne substituents have on the cyclization kinetics, energetics, and reaction pathways of highly conjugated arenediynes. These studies include [*b*]-fused 5,6-diethynylquinoxaline derivatives to further explore how the orientation of extended benzannelation influences enediyne cyclization under thermal and photochemical conditions.

EXPERIMENTAL SECTION

General Procedures. All reagents and solvents were obtained from commercial suppliers and used without further purification. 1,2-Diethynylbenzene (**2**),[40] 1,2-diiodo-4,5-dinitrobenzene (**3**)[41] and porphyrin-2,3-dione **6g**[42] were prepared as described in the literature. Air-sensitive reactions were performed under an inert atmosphere of argon. TLC was performed on precoated silica plates and visualized with short- and long-wavelength UV light. Flash chromatography was conducted with 230–400 mesh silica gel packed in glass columns with the indicated solvent system. Thermolysis reactions were conducted in an oil bath equipped with a temperature controller. Melting points were determined in open capillary tubes on a melting point apparatus and are uncorrected. ^{1}H and ^{13}C NMR spectra were recorded at 500 or 300 MHz and are reported in parts per million relative to tetramethylsilane (0.0 ppm) for ^{1}H or $CDCl_3$ (77.0 ppm) for ^{13}C. IR spectra of all solids were obtained as potassium bromide pellets. UV–vis absorbance and emission spectra were obtained on air-equilibrated CH_2Cl_2 solutions at 20–25 °C. DSC data were collected on neat solid samples. Mass spectra were recorded using electrospray ionization with a time-of-flight mass analyzer.

Computational Methodology. Calculations were carried out using the Gaussian 03 quantum chemistry program.[43] Geometry optimizations were carried out using the mPW1PW91[44,45] density functional and 6-31G(d,p) basis set. Single-point energies for all optimized geometries were obtained with the mPW1PW91 density functional and cc-pVTZ basis set. The mPW1PW91 density functional was chosen for its ability to accurately reproduce the crystal structure of arenediynes.[46] Calculations for the closed-shell reactant enediynes utilized restricted wave functions, whereas calculations for the open-shell transition states and diradical products for the Bergman cyclization reactions utilized broken-symmetry unrestricted wave functions.[17,47] For the transition states and diradical products, both singlet and triplet states were calculated; in all cases, the singlet states proved to be lower in energy (Table S1, Supporting Information), and the singlet states were subsequently used exclusively in the calculation of the enthalpy barrier and reaction enthalpy in Tables 4 and 5, while free energies of activation and reaction for the Bergman cyclization are provided in Table S2 (Supporting Information). Vibrational frequency calculations were used to verify each optimized structure as a stationary point as well as to obtain free energies for all species. Solvation energies were obtained using the IEF-PCM (integral equation formalism polarized continuum model) implicit solvent model with benzene, 2-propanol, and acetonitrile as solvents. Because the reaction thermodynamics for cyclization do not appreciably change when solvation energies are included, the discussion is focused on gas-phase energetics, while the energetics in solvent are given in the Supporting Information (Tables S3 and S4).

1,2-Bis[(trimethylsilyl)ethynyl]-4,5-dinitrobenzene (4). To a degassed solution of 1,2-diiodo-4,5-dinitrobenzene (2.5 g, 6.0 mmol) in Et_3N (60 mL) was added $Pd(PPh_3)_4$ (0.138 g, 0.12 mmol) followed by (trimethylsilyl)acetylene (1.75 g, 18.0 mmol) and CuI (0.068 g, 0.36 mmol). After being stirred in the dark for 12 h under argon, the reaction was diluted with Et_2O, washed with saturated aqueous NH_4Cl and NaCl, dried (Na_2SO_4), and evaporated in vacuo. The resulting solid was purified by silica gel chromatography (9:1 hexanes/ethyl acetate) and recrystallized from ethanol to give the title compound as a yellow solid (1.65 g, 76%): mp 84–86 °C; ^{1}H NMR (300 MHz, $CDCl_3$) δ 0.30 (s, 18H), 7.94 (s, 2H); ^{13}C NMR (75 MHz, $CDCl_3$) δ −0.4, 99.3, 107.5, 128.4, 131.0, 141.2; IR (KBr, cm^{-1}) 2154, 1542, 1353, 876; UV–vis (CH_2Cl_2) λ_{max} (nm) (log ε) 314 (4.07), 269 (4.42); HRMS (ES) *m*/*z* calcd for $C_{16}H_{20}N_2O_4Si_2$ $[M + Na]^+$ 383.0859, found 383.0857.

4,5-Bis[(trimethylsilyl)ethynyl]-1,2-diaminobenzene (5). To a solution of **4** (0.25 g, 0.69 mmol) in absolute EtOH (25 mL) were added AcOH (2.5 mL) and zinc dust (1.0 g). After being stirred for 10 min, the solution was filtered, diluted with Et_2O, and washed with water, saturated aqueous $NaHCO_3$, and NaCl, dried (Na_2SO_4), and evaporated in vacuo. The resulting solid was purified by silica gel chromatography (3:2 hexanes/ethyl acetate) to give the title compound as a white solid (0.206 g, 99%): mp 117–119 °C; ^{1}H NMR (300 MHz, $CDCl_3$) δ 0.24 (s, 18H), 3.45 (br s, 4H), 6.78 (s, 2H); ^{13}C NMR (75 MHz, $CDCl_3$) δ 0.2, 95.4, 103.9, 117.8, 119.7, 135.0; IR (KBr, cm^{-1}) 3388, 3327, 2140, 833; UV–vis (CH_2Cl_2) λ_{max} (nm) (log ε) 307 (4.22), 262 (4.80); HRMS (ES) *m*/*z* calcd for $C_{16}H_{24}N_2Si_2$ $[M + Na]^+$ 323.1376, found 323.1374.

6,7-Bis[(trimethylsilyl)ethynyl]quinoxaline (7a). To a mixture of 40% glyoxal in water (0.10 g, 0.69 mmol) and benzene (10 mL) was added diamine **5** (0.19 g, 0.63 mmol), and the resulting mixture was vigorously stirred in the dark for 12 h. The solvent was removed in vacuo, and the resulting solid was purified by silica gel chromatography (7:3 hexanes/ethyl acetate) to give **7a** as a tan solid (0.14 g, 70%): mp 86–88 °C; ^{1}H NMR (300 MHz, $CDCl_3$) δ 0.32 (s, 18H), 8.20 (s, 2H), 8.80 (s, 2H); ^{13}C NMR (75 MHz, $CDCl_3$) δ −0.08, 101.3, 101.9, 126.9, 133.5, 142.2, 145.8; IR (KBr, cm^{-1}) 2157, 832; UV–vis (CH_2Cl_2) λ_{max} (nm) (log ε) 369 (3.84), 352 (3.79); HRMS (ES) *m*/*z* calcd for $C_{18}H_{22}N_2Si_2$ $[M + H]^+$ 323.1400, found 323.1406.

9,10-Bis[(trimethylsilyl)ethynyl]acenaphtho[1,2-*b*]-quinoxaline (7b). To a solution of acenaphthenequinone (0.089 g, 0.49 mmol) in benzene (60 mL) was added diamine **5** (0.15 g, 0.50

dx.doi.org/10.1021/jo302009c | J. Org. Chem. 2012, 77, 10329–10339

mmol), and the reaction mixture was refluxed in the dark for 3 days. The solvent was removed in vacuo, and the resulting solid was purified by silica gel chromatography (ethyl acetate) to give **7b** as a tan solid (0.19 g, 89%): mp 209−210 °C; ^{1}H NMR (300 MHz, $CDCl_3$) δ 0.35 (s, 18H), 7.81 (t, J = 7.7 Hz, 2H), 8.08 (d, J = 8.2 Hz, 2H), 8.24 (s, 2H), 8.35 (d, J = 7.3 Hz, 2H); ^{13}C NMR (75 MHz, $CDCl_3$) δ 0.4, 100.5, 102.5, 122.2, 125.8, 128.7, 129.8, 129.9, 131.3, 133.5, 136.7, 140.5 154.8; IR (KBr, cm^{-1}) 2154, 842; UV−vis (CH_2Cl_2) λ_{max} (nm) (log ε) 407 (4.18), 386 (4.35), 366 (4.58), 335 (5.08), 323 (4.96), 286 (4.82), 268 (4.82); HRMS (ES) m/z calcd for $C_{28}H_{26}N_2Si_2$ $[M + Na]^+$ 469.1532, found 469.1531.

9,10-Bis[(trimethylsilyl)ethynyl]benzo[*a*]phenazine (7c). To a solution of 1,2-naphthoquinone (0.085 g, 0.54 mmol) in benzene (68 mL) was added diamine **5** (0.17 g, 0.56 mmol), and the reaction mixture was stirred in the dark for 3 days. The solvent was removed in vacuo, and the resulting solid was purified by silica gel chromatography (3:2 hexanes/ethyl acetate) to give **7c** as a brown solid (0.14 g, 60%): mp 190−192 °C; ^{1}H NMR (300 MHz, $CDCl_3$) δ 0.348 (s, 9H), 0.353 (s, 9H), 7.75−7.78 (m, 2H), 7.86−7.89 (m, 2H), 7.97 (d, J = 9.3 Hz, 1H), 8.35 (s, 1H), 8.45 (s, 1H), 9.28−9.31 (m, 1H); ^{13}C NMR (75 MHz, $CDCl_3$) δ −0.03, 101.3, 101.4, 102.47, 102.52, 125.5, 126.2, 126.3, 127.1, 128.1, 128.3, 130.2, 131.0, 133.3, 133.4, 133.8, 133.9, 141.1, 142.0, 143.3, 144.4; IR (KBr, cm^{-1}) 2152, 840; UV−vis (CH_2Cl_2) λ_{max} (nm) (log ε) 432 (4.55), 408 (4.36), 306 (5.13); HRMS (ES) m/z calcd for $C_{26}H_{26}N_2Si_2$ $[M + H]^+$ 423.1713, found 423.1714.

11,12-Bis[(trimethylsilyl)ethynyl]dibenzo[*a*,*c*]phenazine (7d). To a solution of 9,10-phenanthrenequinone (0.11 g, 0.52 mmol) in benzene (60 mL) was added diamine **5** (0.15 g, 0.48 mmol), and the reaction mixture was refluxed in the dark for 3 days. The solvent was removed in vacuo, and the resulting solid was purified by silica gel chromatography (3:2 hexanes/ethyl acetate) to give **7d** as a yellow solid (0.22 g, 95%): mp 218−220 °C; ^{1}H NMR (300 MHz, $CDCl_3$) δ 0.36 (s, 18H), 7.68−7.80 (m, 4H), 8.40 (s, 2H), 8.50 (d, J = 7.9 Hz, 2H), 9.27 (dd, J = 8.0, 1.5 Hz, 2H); ^{13}C NMR (75 MHz, $CDCl_3$) δ 0.01, 101.0, 102.6, 122.9, 126.1, 126.4, 128.0, 130.0, 130.6, 132.2, 133.5, 141.3, 143.2; IR (KBr, cm^{-1}) 2153, 843; UV−vis (CH_2Cl_2) λ_{max} (nm) (log ε) 426 (4.75), 402 (4.55), 307 (4.96); HRMS (ES) m/z calcd for $C_{30}H_{28}N_2Si_2$ $[M + H]^+$ 473.1869, found 473.1872.

11,12-Bis[(trimethylsilyl)ethynyl]dipyrido[3,2-*a*:2′,3′-*c*]phenazine (7e). To a solution of 1,10-phenanthroline-5,6-dione (0.10 g, 0.49 mmol) in benzene (60 mL) was added diamine **5** (0.15 g, 0.48 mmol), and the reaction mixture was refluxed in the dark for 3 days. The solvent was removed in vacuo, and the resulting solid was purified by recrystallization (ethanol) to give **7e** as a yellow solid (0.20 g, 89%): mp 286−289 °C dec; ^{1}H NMR (300 MHz, $CDCl_3$) δ 0.37 (s, 18H), 7.75 (dd, J = 8.2, 4.5 Hz, 2H), 8.40 (s, 2H), 9.24 (dd, J = 4.4, 1.9 Hz, 2H), 9.45 (dd, J = 8.1, 1.8 Hz, 2H); ^{13}C NMR (75 MHz, $CDCl_3$) δ 0.09, 102.1, 102.2, 124.2, 127.1, 127.2, 133.4, 133.8, 141.5, 141.8, 148.4, 152.8; IR (KBr, cm^{-1}) 2156, 855; UV−vis (CH_2Cl_2) λ_{max} (nm) (log ε) 418 (4.69), 395 (4.50), 304 (5.00); HRMS (ES) m/z calcd for $C_{28}H_{26}N_4Si_2$ $[M + H]^+$ 475.1774, found 475.1765.

13,14-Bis[(trimethylsilyl)ethynyl]benzo[*a*]naphtho[2,1-*c*]phenazine (7f). To a solution of 11,12-dihydrochrysene-11,12-dione (0.19 g, 0.73 mmol) in benzene (88 mL) was added diamine **5** (0.22 g, 0.73 mmol), and the reaction mixture was refluxed in the dark for 3 days. The solvent was removed in vacuo, and the resulting solid was purified by silica gel chromatography (toluene) to give **7f** as a yellow solid (0.32 g, 85%): mp 261−264 °C dec; ^{1}H NMR (300 MHz, $CDCl_3$) δ 0.365 (s, 9H), 0.371 (s, 9H), 7.68 (td, J = 7.6, 1.2 Hz, 1H), 7.76−7.88 (m, 3H), 8.01 (d, J = 7.6 Hz, 1H), 8.19 (d, J = 8.7 Hz, 1H), 8.48 (s, 1H), 8.58 (s, 1H), 8.65 (d, J = 8.9 Hz, 2H), 9.42 (dd, J = 7.8, 1.7 Hz, 1H), 10.91 (d, J = 8.7 Hz, 1H); ^{13}C NMR (75 MHz, C_6D_6) δ 0.18, 0.21, 100.88, 100.93, 103.8, 103.9, 121.0, 123.9, 124.9, 126.2, 126.4, 126.6, 126.7, 128.8, 130.5, 130.8, 131.1, 132.2, 132.6, 132.7, 132.9, 133.9, 134.1, 134.2, 139.9, 140.5, 143.3, 145.5 (two ^{13}C resonances obscured by C_6D_6 solvent peaks); IR (KBr, cm^{-1}) 2154, 843; UV−vis (CH_2Cl_2) λ_{max} (nm) (log ε) 444 (4.28), 420 (4.21), 334 (4.54); HRMS (ES) m/z calcd for $C_{34}H_{30}N_2Si_2$ $[M + H]^+$ 523.2026, found 523.2029.

5,10,15,20-Tetraphenyl-24,25-bis[(trimethylsilyl)ethynyl]quinoxalino[2,3-*b*]porphyrin (7g). Diamine **5** (0.15 g, 0.5 mmol) was added to a solution of porphyrin-2,3-dione (0.32 g, 0.5 mmol) in CH_2Cl_2 (60 mL), and the resulting mixture was stirred in the dark for 48 h. The solvent was removed in vacuo, and the resulting solid was purified by silica gel chromatography (1:1 hexanes/CH_2Cl_2) and recrystallized from CH_2Cl_2/hexanes to give porphyrenediyne **7g** as a purple solid (417 mg, 90%): mp > 250 °C; ^{1}H NMR (300 MHz, $CDCl_3$) δ −2.58 (br s, 2H), 0.37 (s, 18H), 7.74−7.81 (m, 10H), 7.92 (t, J = 7.5 Hz, 2H), 7.98 (s, 2H), 8.13 (d, J = 7.0 Hz, 4H), 8.22 (d, J = 7.6 Hz, 4H), 8.72 (s, 2H), 8.92 (d, J = 4.8 Hz, 2H), 8.94 (d, J = 5.1 Hz, 2H); ^{13}C NMR (75 MHz, $CDCl_3$) δ 0.1, 100.5, 102.9, 117.3, 121.8, 125.7, 126.8, 126.9, 127.8, 127.9, 128.0, 128.3, 133.8, 134.2, 134.4, 134.7, 138.1, 139.6, 140.0, 141.6, 141.8, 145.2, 153.2, 155.1; UV−vis (CH_2Cl_2) λ_{max} (nm) (log ε) 423 (5.31), 530 (4.31), 601 (4.09); UV−vis (TFA−CH_2Cl_2) λ_{max} (nm) (log ε) 484 (5.29), 700 (4.48); HRMS (FAB) m/z calcd for $C_{60}H_{48}N_6Si_2$ $[M + H]^+$ 909.3557, found 909.3561.

6,7-Diethynylquinoxaline (8a). Silylated quinoxalenediyne **7a** (0.050 g, 0.16 mmol) was dissolved in a mixture of THF (20 mL) and a saturated solution of K_2CO_3 in MeOH (5 mL), and the reaction was stirred for 1 h. Upon completion, the reaction was diluted with CH_2Cl_2, washed with water and saturated aqueous NaCl, dried (Na_2SO_4), and evaporated in vacuo. The residue was purified by silica gel chromatography (3:1 hexanes/ethyl acetate) to give quinoxalenediyne **8a** as a tan solid (0.027 g, 98%): mp 175−176 °C dec; ^{1}H NMR (300 MHz, $CDCl_3$) δ 3.44 (s, 2H), 8.20 (s, 2H), 8.78 (s, 2H); ^{13}C NMR (75 MHz, $CDCl_3$) δ 80.7, 83.4, 126.0, 134.1, 142.3, 146.1; IR (KBr, cm^{-1}) 3271, 2097; UV−vis (CH_2Cl_2) λ_{max} (nm) (log ε) 358 (3.66), 342 (3.67), 261 (4.64); Em (CH_2Cl_2) λ_{max} (nm) 381; HRMS (ES) m/z calcd for $C_{12}H_6N_2$ $[M + H]^+$ 179.0609, found 179.0602; DSC onset 178 °C, T_{max} = 189 °C.

9,10-Diethynylacenaphtho[1,2-*b*]quinoxaline (8b). Silylated acenaphthoquinoxalenediyne **7b** (0.106 g, 0.24 mmol) was dissolved in a mixture of THF (50 mL) and a saturated solution of K_2CO_3 in MeOH (18 mL), and the reaction was stirred for 1 h. Upon completion, the reaction was diluted with CH_2Cl_2, washed with water and saturated aqueous NaCl, dried (Na_2SO_4), and evaporated in vacuo. The residue was then filtered through a short plug of silica gel (CH_2Cl_2) to give acenaphthoquinoxalenediyne **8b** as a tan solid (0.071 g, 98%): mp 201−202 °C dec; ^{1}H NMR (500 MHz, $CDCl_3$) δ 3.51 (s, 2H), 7.88 (dd, J = 8.2, 7.0 Hz, 2H), 8.16 (d, J = 8.3 Hz, 2H), 8.37 (s, 2H), 8.45 (d, J = 7.1 Hz, 2H); ^{13}C NMR (125 MHz, $CDCl_3$) δ 81.3, 82.7, 122.5, 124.9, 128.8, 130.1, 131.3, 134.2, 137.0, 140.8, 155.2; IR (KBr, cm^{-1}) 3291, 2103; UV−vis (CH_2Cl_2) λ_{max} (nm) (log ε) 400 (3.72), 380 (4.02), 361 (4.22), 331 (4.80), 318 (4.64), 281 (4.41), 241 (4.77); Em (CH_2Cl_2) λ_{max} (nm) 405, 427; HRMS (ES) m/z calcd for $C_{22}H_{10}N_2$ $[M + H]^+$ 303.0922, found 303.0925; DSC onset 194 °C, T_{max} = 209 °C.

9,10-Diethynylbenzo[*a*]phenazine (8c). Silylated naphthoquinoxalenediyne **7c** (0.11 g, 0.26 mmol) was dissolved in a mixture of THF (20 mL) and a saturated solution of K_2CO_3 in MeOH (5 mL), and the reaction was stirred for 1 h. Upon completion, the reaction was diluted with CH_2Cl_2, washed with water and saturated aqueous NaCl, dried (Na_2SO_4), and evaporated in vacuo. The residue was then filtered through a short plug of silica gel (CH_2Cl_2) to give naphthoquinoxalenediyne **8c** as a brown solid (0.067 g, 93%): mp 166−168 °C dec; ^{1}H NMR (500 MHz, $CDCl_3$) δ 3.45 (s, 1H), 3.55 (s, 1H), 7.81−7.82 (m, 2H), 7.91−7.93 (m, 2H), 8.04 (d, J = 9.0 Hz, 1H), 8.45 (s, 1H), 8.54 (s, 1H), 9.36 (dd, J = 9.5, 4.0 Hz, 1H); ^{13}C NMR (125 MHz, $CDCl_3$) δ 81.2, 83.36, 83.38, 125.2, 125.4, 125.7, 127.0, 128.3, 128.4, 130.4, 130.9, 133.5, 133.9, 134.3, 134.4, 141.1, 141.9, 143.6, 144.6; IR (KBr, cm^{-1}) 3271, 2106; UV−vis (CH_2Cl_2) λ_{max} (nm) (log ε) 426 (4.18), 403 (4.08), 382 (3.94), 300 (4.71); Em (CH_2Cl_2) λ_{max} (nm) 439, 459; HRMS (ES) m/z calc′d for $C_{20}H_{10}N_2$ $[M + H]^+$ 279.0922, found 279.0918; DSC onset 173 °C, T_{max} = 197 °C.

11,12-Diethynyldibenzo[*a*,*c*]phenazine (8d). Silylated phenanthroquinoxalenediyne **7d** (0.12 g, 0.25 mmol) was dissolved in a mixture of THF (30 mL) and a saturated solution of K_2CO_3 in MeOH (20 mL), and the reaction was stirred for 1 h. Upon completion, the reaction was diluted with CH_2Cl_2, washed with water and saturated aqueous NaCl, dried (Na_2SO_4), and evaporated in vacuo. The residue was then filtered through a short plug of silica gel (CH_2Cl_2) to give phenanthroquinoxalenediyne **8d** as a yellow solid (0.042 g, 51%): mp 166−167 °C dec; ^{1}H

NMR (500 MHz, $CDCl_3$) δ 3.57 (s, 2H), 7.78 (td, J = 7.5, 1.0 Hz, 2H), 7.86 (td, J = 7.5, 1.5 Hz, 2H), 8.54 (s, 2H), 8.60 (d, J = 8.1 Hz, 2H), 9.39 (dd, J = 8.0, 1.4 Hz, 2H); ^{13}C NMR (125 MHz, $CDCl_3$) δ 81.3, 83.1, 123.0, 125.2, 126.6, 128.2, 129.9, 131.0, 132.4, 134.1, 141.4, 143.6; IR (KBr, cm^{-1}) 3283, 2106; UV−vis (CH_2Cl_2) λ_{max} (nm) (log ε) 419 (4.52), 396 (4.33), 376 (4.03), 317 (4.44), 304 (4.70), 267 (4.78); Em (CH_2Cl_2) λ_{max} (nm) 426, 449; HRMS (ES) m/z calcd for $C_{24}H_{12}N_2$ [M + H]$^+$ 329.1078, found 329.1078; DSC onset 164 °C, T_{max} = 174 °C.

11,12-Diethynyldipyrido[3,2-*a*:2′,3′-*c*]phenazine (8e). Silylated phenanthrolinoquinoxalenediyne **7e** (0.10 g, 0.21 mmol) was dissolved in a mixture of THF (50 mL) and a saturated solution of K_2CO_3 in MeOH (17 mL), and the reaction was stirred for 1 h. Upon completion, the reaction was diluted with CH_2Cl_2, washed with water and saturated aqueous NaCl, dried (Na_2SO_4), and evaporated in vacuo. The residue was then filtered through a short plug of silica gel (CH_2Cl_2) to give phenanthrolinoquinoxalenediyne **8e** as a yellow solid (0.049 g, 70%): mp 214−215 °C dec; ^{1}H NMR (500 MHz, $CDCl_3$) δ 3.59 (s, 2H), 7.79 (dd, J = 8.1, 4.5 Hz, 2H), 8.50 (s, 2H), 9.28 (dd, J = 4.4, 1.8 Hz, 2H), 9.55 (d, J = 8.1 Hz, 2H); ^{13}C NMR (125 MHz, $CDCl_3$) δ 81.0, 84.0, 124.3, 126.2, 127.2, 134.0, 134.1, 141.6, 142.2, 148.6, 153.0; IR (KBr, cm^{-1}) 3292, 2100; UV−vis (CH_2Cl_2) λ_{max} (nm) (log ε) 408 (4.50), 397 (4.16), 386 (4.31), 376 (4.09), 366 (4.07), 296 (4.81); Em (CH_2Cl_2) λ_{max} (nm) 414, 437; HRMS (ES) m/z calcd for $C_{22}H_{10}N_4$ [M + H]$^+$ 331.0983, found 331.0980; DSC onset 200 °C, T_{max} = 214 °C.

13,14-Diethynylbenzo[*a*]naphtho[2,1-*c*]phenazine (8f). Silylated chrysenoquinoxalenediyne **7f** (0.227 g, 0.44 mmol) was dissolved in a mixture of THF (20 mL) and a saturated solution of K_2CO_3 in MeOH (38 mL), and the reaction was stirred for 1 h. Upon completion, the reaction was diluted with CH_2Cl_2, washed with water and saturated aqueous NaCl, dried (Na_2SO_4), and evaporated in vacuo. The residue was then filtered through a short plug of silica gel (CH_2Cl_2) to give chrysenoquinoxalenediyne **8f** as a yellow solid (0.148 g, 90%): mp 179−180 °C dec; ^{1}H NMR (500 MHz, $CDCl_3$) δ 3.569 (s, 1H), 3.573 (s, 1H), 7.69 (t, J = 6.5 Hz, 1H), 7.79−7.90 (m, 3H), 8.03 (dd, J = 8.0, 1.0 Hz, 1H), 8.22 (d, J = 9.0 Hz, 1H), 8.54 (s, 1H), 8.65−8.68 (m, 3H), 9.44 (dd, J = 7.5, 1.3 Hz, 1H), 10.88 (d, J = 8.5 Hz, 1H); ^{13}C NMR (125 MHz, $CDCl_3$) δ 81.4, 83.2, 120.9, 123.9, 124.4, 125.1, 125.3, 126.5, 126.6, 128.2, 128.3, 128.7, 130.0, 130.3, 130.9, 132.1, 132.5, 132.6, 133.0, 133.9, 134.0, 134.1, 139.7, 140.4, 143.5, 145.5; IR (KBr, cm^{-1}) 3287, 2103; UV−vis (CH_2Cl_2) λ_{max} (nm) (log ε) 440 (4.26), 417 (4.23), 332 (4.61), 317 (4.53), 287 (4.80), 281 (4.83), 258 (4.72); Em (CH_2Cl_2) λ_{max} (nm) 496; HRMS (ES) m/z calcd for $C_{28}H_{14}N_2$ [M + H]$^+$ 379.1235, found 379.1245; DSC onset 168 °C, T_{max} = 182 °C.

5,10,15,20-Tetraphenyl-24,25-diethynylquinoxalino[2,3-*b*]-porphyrin (8g). Silylated porphyrenediyne **7g** (0.30 g, 0.32 mmol) was dissolved in a mixture of THF (75 mL) and a saturated solution of K_2CO_3 in MeOH (25 mL), and the reaction was stirred for 1 h. Upon completion, the reaction was diluted with CH_2Cl_2, washed with water and saturated aqueous NaCl, dried (Na_2SO_4), and evaporated in vacuo. The residue was recrystallized from CH_2Cl_2/MeOH to give porphyrenediyne **8g** as a purple solid (0.222 g, 90%): mp > 250 °C; ^{1}H NMR (300 MHz, $CDCl_3$) δ −2.60 (br s, 2H), 3.54 (s, 2H), 7.75−7.81 (m, 10H), 7.89 (t, J = 7.4 Hz, 2H), 8.05 (s, 2H), 8.12 (d, J = 7.3 Hz, 4H), 8.21 (d, J = 7.3 Hz, 4H), 8.71 (s, 2H), 8.92 (d, J = 4.9 Hz, 2H), 8.95 (d, J = 4.9 Hz, 2H); ^{13}C NMR (75 MHz, $CDCl_3$) δ 81.6, 82.7, 117.3, 121.8, 124.5, 126.8, 126.9, 127.8, 127.9, 128.1, 128.3, 133.8, 134.3, 134.5, 135.3, 138.1, 139.5, 140.0, 141.5, 141.7, 144.9, 153.2, 155.1; UV−vis (CH_2Cl_2) λ_{max} (nm) (log ε) 421 (5.31), 531 (4.27), 602 (4.08), 652 (3.04); UV−vis (TFA−CH_2Cl_2) λ_{max} (nm) (log ε) 466 (5.20), 483 (5.22), 605 (3.93), 699 (4.56); Em (CH_2Cl_2) λ_{max} (nm) 658, 726; HRMS (FAB) m/z calcd for $C_{54}H_{32}N_6$ [M + H]$^+$ 765.2767, found 765.2770; DSC onset 310 °C, T_{max} = 356 °C.

Benzo[*g*]quinoxaline (9). **8a** (0.039 g, 0.022 mmol) was dissolved in chlorobenzene containing 10% 1,4-cyclohexadiene (20 mL), and the resulting solution was placed in a pressure tube, which was degassed with argon and sealed. The reaction was heated to 180 °C in an oil bath for 24 h. After the reaction was cooled to room temperature, the solvent was evaporated in vacuo to afford a 3:1 mixture of **9** and 5,10-dihydrobenzo[*g*]quinoxaline (**10**). The resulting mixture was dissolved in toluene (20 mL), DDQ was added (0.050 mg, 0.22 mmol), and the solution was refluxed for 16 h. Upon cooling, the solution was diluted with ethyl acetate, washed with saturated aqueous $NaHCO_3$ and NaCl, dried (Na_2SO_4), and evaporated in vacuo. The resulting solid was purified by silica gel chromatography (3:1 dichloromethane/ethyl acetate) to give **9** as an orange solid (0.012 g, 30%): mp 123−124 °C (lit.[48] mp 125−126 °C); ^{1}H NMR (500 MHz, $CDCl_3$) δ 7.60 (dd, J = 6.6, 3.2 Hz, 2H), 8.13 (dd, J = 6.5, 3.3 Hz, 2H), 8.70 (s, 2H), 8.89 (s, 2H); ^{13}C NMR (125 MHz, $CDCl_3$) δ 127.0, 128.0, 128.5, 133.9, 139.4, 145.6; IR (KBr, cm^{-1}) 3030, 1590, 1524; HRMS (ES) m/z calcd for $C_{12}H_8N_2$ [M + H]$^+$ 181.0765, found 181.0760.

10,15-Dihydrotribenzo[*a*,*c*,*i*]phenazine (12). **8d** (0.020 g, 0.061 mmol) was dissolved in chlorobenzene containing 20% 1,4-cyclohexadiene (20 mL), and the resulting solution was placed in a pressure tube, which was degassed with argon and sealed. The reaction was heated to 180 °C in an oil bath for 48 h. After the reaction was cooled to room temperature, the solvent was evaporated in vacuo to afford a 9:1 mixture of **12** and tribenzo[*a*,*c*,*i*]phenazine (**11**). The resulting mixture was purified by column chromatography (4:1 toluene/hexanes) to give **12** as an orange solid (0.013 g, 65%): mp 290−293 °C; ^{1}H NMR (300 MHz, $CDCl_3$) δ 4.48 (s, 4H), 7.30 (dd, J = 5.6, 3.3 Hz, 2H), 7.44 (dd, J = 5.4, 3.4 Hz, 2H), 7.70−7.80 (m, 4H), 8.61−8.64 (m, 2H), 9.25−9.28 (m, 2H); ^{13}C NMR (75 MHz, $CDCl_3$) δ 38.6, 122.7, 125.1, 126.8, 127.5, 128.1, 128.9, 130.0, 131.1, 134.6, 139.0, 150.7; IR (KBr, cm^{-1}) 3051, 2925, 2850, 1608, 1495; HRMS (ES) m/z calcd for $C_{24}H_{16}N_2$ [M + H]$^+$ 333.1391, found 333.1396.

5,10,15,20-Tetraphenylbenzoquinoxalino[2,3-*b*]porphyrin (13). Porphyrenediyne **8g** (0.019 g, 0.025 mmol) was dissolved in chlorobenzene containing 20% (v/v) 1,4-cyclohexadiene (15 mL), and the resulting solution was placed in a pressure tube, which was degassed with argon and sealed. The reaction was heated to 180 °C in an oil bath for 24 h. After the reaction was cooled to room temperature, the solvent was evaporated in vacuo and the resulting solid purified by silica gel chromatography (3:1 hexanes/CH_2Cl_2) and recrystallized from CH_2Cl_2/MeOH to give **13** as a purple solid (0.0175 g, 92%): mp > 250 °C; ^{1}H NMR (300 MHz, $CDCl_3$) δ −2.43 (br s, 2H), 7.56 (dd, J = 6.7, 3.0 Hz, 2H), 7.74−7.85 (m, 10H), 7.95 (t, J = 7.6 Hz, 2H), 8.15 (dd, J = 6.4, 3.4 Hz, 2H), 8.18−8.23 (m, 8H), 8.47 (s, 2H), 8.68 (s, 2H), 8.90 (d, J = 4.4 Hz, 2H), 8.93 (d, J = 5.0 Hz, 2H); ^{13}C NMR (75 MHz, $CDCl_3$) δ 116.4, 121.9, 126.2, 126.8, 127.0, 127.7, 127.8, 127.9, 128.0, 128.5, 128.8, 133.7, 133.9, 134.0, 134.4, 137.7, 137.8, 139.8, 141.8, 141.9, 146.1, 153.3, 154.8; UV−vis (CH_2Cl_2) λ_{max} (nm) (log ε) 426 (5.34), 533 (4.58), 608 (4.36), 660 (3.98); UV−vis (TFA−CH_2Cl_2) λ_{max} (nm) (log ε) 422 (4.99), 459 (5.17), 503 (4.95), 626 (4.40), 711 (4.63); HRMS (FAB) calcd for $C_{54}H_{34}N_6$ [M + H]$^+$ 767.2923, found 767.2921.

■ ASSOCIATED CONTENT

Supporting Information

^{1}H NMR and ^{13}C NMR spectra of **4**, **5**, **7a**−**7g**, **8a**−**8g**, **9**, **12**, and **13**, absorbance and emission spectra of **8a**−**8g**, computational details (singlet−triplet energy gaps, free energy changes for cyclization, and reaction energies in solvent), and Cartesian coordinates for geometry-optimized structures. This material is available free of charge via the Internet at http://pubs.acs.org.

■ AUTHOR INFORMATION

Corresponding Author

*E-mail: jspence@csus.edu (J.D.S.); ghermanb@csus.edu (B.F.G.).

Notes

The authors declare no competing financial interest.

■ ACKNOWLEDGMENTS

Funding for this project has been provided by the donors of the Petroleum Research Fund, administered by the American Chemical Society (Grant 47422-B4), the National Science Foundation (Grant CHE-0922676), the California State University Program in Education and Research in Biotechnology

(CSUPERB), and the California State University, Sacramento, Research and Creative Activity (RCA) and Summer Undergraduate Research Experience (SURE) programs.

REFERENCES

(1) (a) Jones, R. R.; Bergman, R. G. *J. Am. Chem. Soc.* **1972**, *94*, 660. (b) Bergman, R. G. *Acc. Chem. Res.* **1973**, *6*, 25.

(2) (a) Koga, N.; Morokuma, K. *J. Am. Chem. Soc.* **1991**, *113*, 1907. (b) Galbraith, J. M.; Schreiner, P. R.; Harris, N.; Wei, W.; Wittkopp, A.; Shaik, S. *Chem.—Eur. J.* **2000**, *6*, 1446. (c) Alabugin, I. V.; Manoharan, M. *J. Phys. Chem. A* **2003**, *107*, 3363.

(3) (a) Stahl, F.; Moran, D.; Schleyer, P. v. R.; Prall, M.; Schreiner, P. R. *J. Org. Chem.* **2002**, *67*, 1453. (b) De Proft, F.; Schleyer, P. v. R.; Lenthe, J. H. v.; Stahl, F.; Geerlings, P. *Chem.—Eur. J.* **2002**, *8*, 3402.

(4) (a) Nicolaou, K. C.; Dai, W.-M. *Angew. Chem., Int. Ed. Engl.* **1991**, *30*, 1387. (b) Nicolaou, K. C.; Smith, A. L. *Acc. Chem. Res.* **1992**, *25*, 497. (c) Maier, M. E. *Synlett* **1995**, 13. (d) Maier, M. E.; Bosse, F.; Niestroj, A. *Eur. J. Org. Chem.* **1999**, 1. (e) Grissom, J. W.; Gunawardena, G. U.; Klingberg, D.; Huang, D. H. *Tetrahedron* **1996**, *52*, 6453. (f) Wang, K. K. *Chem. Rev.* **1996**, *96*, 207.

(5) (a) Galm, U.; Hager, M. H.; Van Lanen, S. G.; Ju, J.; Thorson, J. S.; Shen, B. *Chem. Rev.* **2005**, *105*, 739. (b) *Enediyne Antibiotics as Antitumor Agents*; Borders, D. B., Doyle, T. W., Eds.; Marcel Dekker: New York, 1995. (c) *Neocarzinostatin: The Past, Present, and Future of an Anticancer Drug*; Maeda, H., Edo, K., Ishida, N., Eds.; Springer: New York, 1997.

(6) (a) Bowles, D. M.; Anthony, J. E. *Org. Lett.* **2000**, *2*, 85. (b) Chow, S.-Y.; Palmer, G. J.; Bowles, D. M.; Anthony, J. E. *Org. Lett.* **2000**, *2*, 961. (c) Bowles, D. M.; Palmer, G. J.; Landis, C. A.; Scott, J. L.; Anthony, J. E. *Tetrahedron* **2001**, *57*, 3753.

(7) Gulevskaya, A. V.; Tyaglivy, A. S. *Chem. Heterocycl. Compd.* **2012**, *48*, 82.

(8) (a) Whitlock, H. W., Jr.; Sandvick, P. E.; Overman, L. E.; Reichardt, P. B. *J. Am. Chem. Soc.* **1969**, *34*, 879. (b) Schreiner, P. R.; Prall, M.; Lutz, V. *Angew. Chem., Int. Ed.* **2003**, *42*, 5757.

(9) (a) Scott, J. L; Parkin, S. R.; Anthony, J. E. *Synlett* **2004**, 161. (b) Kovalenko, S. V.; Peabody, S.; Manoharan, M.; Clark, R. J.; Alabugin, I. V. *Org. Lett.* **2004**, *6*, 2457. (c) Peabody, S. W.; Breiner, B.; Kovalenko, S. V.; Patil, S.; Alabugin, I. V. *Org. Biomol. Chem.* **2005**, *3*, 218. (d) Alabugin, I. V.; Gilmore, K.; Patil, S.; Manoharan, M.; Kovalenko, S. V.; Clark, R. J.; Ghiviriga, I. *J. Am. Chem. Soc.* **2008**, *130*, 11535. (e) Byers, P. M.; Alabugin, I. V. *J. Am. Chem. Soc.* **2012**, *134*, 9609.

(10) Lee, C.-Y.; Wu, M.-J. *Eur. J. Org. Chem.* **2007**, 3463.

(11) (a) Marsden, J. A.; Miller, J. J.; Shirtcliff, L. D.; Haley, M. M. *J. Am. Chem. Soc.* **2005**, *127*, 2464. (b) Spitler, E. L.; Shirtcliff, L. D.; Haley, M. M. *J. Org. Chem.* **2007**, *72*, 86. (c) Sugiyama, Y.; Shinohara, Y.; Momotake, A.; Takahashi, K.; Kanna, Y.; Nishimura, Y.; Arai, T. *J. Phys. Chem. A* **2010**, *114*, 10929.

(12) (a) Rule, J. D.; Moore, J. S. *Macromolecules* **2005**, *38*, 7266. (b) Rule, J. D.; Wilson, S. R.; Moore, J. S. *J. Am. Chem. Soc.* **2003**, *125*, 12992.

(13) (a) John, J. A.; Tour, J. M. *J. Am. Chem. Soc.* **1994**, *116*, 5011. (b) Smith, D. W., Jr.; Babb, D. A.; Snelgrove, R. V.; Townsend, P. H., III; Martin, S. J. *J. Am. Chem. Soc.* **1998**, *120*, 9078. (c) Shah, H. V.; Babb, D. A.; Smith, D. W., Jr. *Polymer* **2000**, *41*, 4415. (d) Chen, X.; Tolbert, L. M.; Hess, D. W.; Henderson, C. *Macromolecules* **2001**, *34*, 4104. (e) Perera, K. P. U.; Krawiec, M.; Smith, D. W., Jr. *Tetrahedron* **2002**, *58*, 10197. (f) Johnson, J. P.; Bringley, D. A.; Wilson, E. E.; Lewis, K. D.; Beck, L. W.; Matzger, A. J. *J. Am. Chem. Soc.* **2003**, *125*, 14708.

(14) Sherer, E. C.; Kirschner, K. N.; Pickard, F. C., IV; Rein, C.; Feldgus, S.; Shields, G. C. *J. Phys. Chem. B* **2008**, *112*, 16917 and references therein.

(15) Roth, W. R.; Hopf, H.; Horn, C. *Chem. Ber.* **1994**, *127*, 1765.

(16) Roth, W. R.; Hopf, H.; Wasser, T.; Zimmermann, H.; Werner, C. *Liebigs Ann.* **1996**, 1691.

(17) Prall, M.; Wittkopp, A.; Schreiner, P. R. *J. Phys. Chem. A* **2001**, *105*, 9265.

(18) The actual increase in reaction enthalpy from **1** to **2**, however, is smaller than that predicted from aromatic stabilization energy evaluations. See ref 3a.

(19) Koseki, S.; Fujimura, Y.; Hirama, M. *J. Phys. Chem. A* **1999**, *103*, 7672.

(20) Kaneko, T.; Takahashi, M.; Hirama, M. *Tetrahedron Lett.* **1999**, *40*, 2015.

(21) Lockhart, T. P.; Comita, P. B.; Bergman, R. G. *J. Am. Chem. Soc.* **1981**, *103*, 4082.

(22) Choy, N.; Kim, C. S.; Ballestero, C.; Artigas, L.; Diez, C.; Lichtenberg, F.; Shapiro, J.; Russell, K. C. *Tetrahedron Lett.* **2000**, *41*, 6955.

(23) (a) Alabugin, I. V.; Manoharan, M.; Kovalenko, S. V. *Org. Lett.* **2002**, *4*, 1119. (b) Zeidan, T. A.; Manoharan, M.; Alabugin, I. V. *J. Org. Chem.* **2006**, *71*, 954. (c) Zeidan, T. A.; Kovalenko, S. V.; Manoharan, M.; Alabugin, I. V. *J. Org. Chem.* **2006**, *71*, 962. (d) Pickard, F. C., IV; Shepherd, R. L.; Gillis, A. E.; Dunn, M. E.; Feldgus, S.; Kirschner, K. N.; Shields, G. C.; Manoharan, M.; Alabugin, I. V. *J. Phys. Chem. A* **2006**, *110*, 2517.

(24) (a) Nicolaou, K. C.; Zuccarello, G.; Ogawa, Y.; Schweiger, E. J.; Kumazawa, T. J. *J. Am. Chem. Soc.* **1988**, *110*, 4866. (b) Schreiner, P. R. *J. Am. Chem. Soc.* **1998**, *120*, 4184.

(25) (a) Magnus, P.; Carter, P. A. *J. Am. Chem. Soc.* **1988**, *110*, 1626. (b) Magnus, P.; Lewis, R.; Huffman, J. C. *J. Am. Chem. Soc.* **1988**, *110*, 6921. (c) Snyder, J. P. *J. Am. Chem. Soc.* **1989**, *111*, 7630. (d) Magnus, P.; Fortt, S.; Pitterna, T.; Snyder, J. P. *J. Am. Chem. Soc.* **1990**, *112*, 4986. (e) Magnus, P.; Carter, P.; Elliott, J.; Lewis, R.; Harling, J.; Pitterna, T.; Bauta, W. E.; Fortt, S. *J. Am. Chem. Soc.* **1992**, *114*, 2544.

(26) Funk, R. L.; Young, E. R. R.; Williams, R. M.; Flanagan, M. F.; Cecil, T. L. *J. Am. Chem. Soc.* **1996**, *118*, 3291.

(27) (a) Semmelhack, M. F.; Neu, T.; Foubelo, F. *Tetrahedron Lett.* **1992**, *33*, 3277. (b) Meyers, A. G.; Dragovich, P. S. *J. Am. Chem. Soc.* **1992**, *114*, 5859. (c) Nicolaou, K. C.; Liu, A.; Zeng, Z.; McComb, S. *J. Am. Chem. Soc.* **1992**, *114*, 9279. (d) Semmelhack, M. F.; Neu, T.; Foubelo, F. *J. Org. Chem.* **1994**, *59*, 5038. (e) Poloukhtine, A.; Popik, V. V. *J. Org. Chem.* **2006**, *71*, 7417.

(28) (a) Faust, R.; Weber, C.; Fiandanese, V.; Marchese, G.; Punzi, A. *Tetrahedron* **1997**, *53*, 14655. (b) Kim, C.-S.; Russell, K. C. *J. Org. Chem.* **1998**, *63*, 8229. (c) Kim, C.-S.; Russell, K. C. *Tetrahedron Lett.* **1999**, *40*, 3835. (d) Kim, S.-C.; Diez, C.; Russell, K. C. *Chem.—Eur. J.* **2000**, *6*, 1555. (e) Choy, N.; Blanco, B.; Wen, J.; Krishan, A.; Russell, K. C. *Org. Lett.* **2000**, *2*, 3761. (f) Zhao, Z.; Peng, Y.; Dalley, N. K.; Cannon, J. F.; Peterson, M. A. *Tetrahedron Lett.* **2004**, *45*, 3621. (g) Zhao, Z.; Peacock, J. G.; Gubler, D. A.; Peterson, M. A. *Tetrahedron Lett.* **2005**, *46*, 1373. (h) Vinogradova, O. V.; Balova, I. A.; Popik, V. V. *J. Org. Chem.* **2011**, *76*, 6937.

(29) (a) Aihara, H.; Jaquinod, L.; Nurco, D. J.; Smith, K. M. *Angew. Chem., Int. Ed.* **2001**, *40*, 3439. (b) Nath, M.; Huffman, J. C.; Zaleski, J. M. *Chem. Commun.* **2003**, 858. (c) Chandra, T.; Kraft, B. J.; Huffman, J. C.; Zaleski, J. M. *Inorg. Chem.* **2003**, *42*, 5158. (d) Nath, M.; Huffman, J. C.; Zaleski, J. M. *J. Am. Chem. Soc.* **2003**, *125*, 11484. (e) Spence, J. D.; Cline, E. D.; LLagostera, D. M.; O'Toole, P. S. *Chem. Commun.* **2004**, 180. (f) Nath, M.; Pink, M.; Zaleski, J. M. *J. Am. Chem. Soc.* **2005**, *127*, 478. (g) Nath, M.; Pink, M.; Zaleski, J. M. *J. Organomet. Chem.* **2011**, *696*, 4152. (h) Boerner, L. J. K.; Mazumder, S.; Pink, M.; Baik, M.-H.; Zaleski, J. M. *Chem.—Eur. J.* **2011**, *17*, 14539.

(30) (a) Jones, G. B.; Russell, K. C. The Photo-Bergman Cycloaromatization of Enediynes. In *CRC Handbook of Organic Photochemistry and Photobiology*, 2nd ed.; Horspool, W., Lenci, F., Eds.; CRC Press: Boca Raton, FL, 2004; pp 29−1. (b) Kar, M.; Basak, A. *Chem. Rev.* **2007**, *107*, 2861. (c) Alabugin, I. V.; Yang, W.-Y.; Pal, R. Photochemical Bergman Cyclization and Related Photoreactions of Enediynes. In *CRC Handbook of Organic Photochemistry and Photobiology*, 3rd ed.; Griesbeck, A., Oelgemoller, M., Ghetti, F., Eds.; CRC Press: Boca Raton, FL, 2012; Vol. *1*, pp 549−592.

(31) Bunz, U. H. F. *Chem.—Eur. J.* **2009**, *15*, 6780.

(32) (a) Sonogashira, K.; Tohda, Y.; Hagihara, N. *Tetrahedron Lett.* **1975**, 4467. (b) Chinchilla, R.; Najera, C. *Chem. Rev.* **2007**, *107*, 874.

(33) Weinkauf, J. R.; Cooper, S. W.; Schweiger, A.; Wamser, C. C. *J. Phys. Chem. A* **2003**, *107*, 3486.
(34) Alabugin, I. V.; Manoharan, M. *J. Am. Chem. Soc.* **2003**, *125*, 4495.
(35) Graefenstein, J.; Hjerpe, A. M.; Kraka, E.; Cremer, D. *J. Phys. Chem. A* **2000**, *104*, 1748.
(36) For experimental data, see ref 28b.
(37) Clar, E. *The Aromatic Sextet*; Wiley: New York, 1972.
(38) Clar, E. *Polycyclic Hydrocarbons*; Academic Press: New York, 1964; Vol. *1*, p 34.
(39) Nicolaou, K. C.; Dai, W.-M.; Hong, Y. P.; Tsay, S.-C.; Baldridge, K. K.; Siegel, J. S. *J. Am. Chem. Soc.* **1993**, *115*, 7944.
(40) Grissom, J. W.; Calkins, T. L.; McMillen, H. A.; Jiang, Y. H. *J. Org. Chem.* **1994**, *59*, 5833.
(41) Youngblood, W. J. *J. Org. Chem.* **2006**, *71*, 3345.
(42) Crossley, M. J.; Burn, P. L. *Chem. Commun.* **1984**, 920.
(43) Frisch, M. J.; Trucks, G. W.; Schlegel, H. B.; Scuseria, G. E.; Robb, M. A.; Cheeseman, J. R.; J. A. Montgomery, J.; Vreven, T.; Kudin, K. N.; Burant, J. C.; Millam, J. M.; Iyengar, S. S.; Tomasi, J.; Barone, V.; Mennucci, B.; Cossi, M.; Scalmani, G.; Rega, N.; Petersson, G. A.; Nakatsuji, H.; Hada, M.; Ehara, M.; Toyota, K.; Fukuda, R.; Hasegawa, J.; Ishida, M.; Nakajima, T.; Honda, Y.; Kitao, O.; Nakai, H.; Klene, M.; Li, X.; Knox, J. E.; Hratchian, H. P.; Cross, J. B.; Bakken, V.; Adamo, C.; Jaramillo, J.; Gomperts, R.; Stratmann, R. E.; Yazyev, O.; Austin, A. J.; Cammi, R.; Pomelli, C.; Ochterski, J. W.; Ayala, P. Y.; Morokuma, K.; Voth, G. A.; Salvador, P.; Dannenberg, J. J.; Zakrzewski, V. G.; Dapprich, S.; Daniels, A. D.; Strain, M. C.; Farkas, O.; Malick, D. K.; Rabuck, A. D.; Raghavachari, K.; Foresman, J. B.; Ortiz, J. V.; Cui, Q.; Baboul, A. G.; Clifford, S.; Cioslowski, J.; Stefanov, B. B.; Liu, G.; Liashenko, A.; Piskorz, P.; Komaromi, I.; Martin, R. L.; Fox, D. J.; Keith, T.; Al-Laham, M. A.; Peng, C. Y.; Nanayakkara, A.; Challacombe, M.; Gill, P. M. W.; Johnson, B.; Chen, W.; Wong, M. W.; Gonzalez, C.; Pople, J. A. *Gaussian 03*, revision D.01; Gaussian, Inc.: Wallingford, CT, 2004.
(44) Adamo, C.; Barone, V. *J. Chem. Phys.* **1998**, *108*, 664.
(45) Perdew, J. P.; Chevary, J. A.; Vosko, S. H.; Jackson, K. A.; Pederson, M. R.; Singh, D. J.; Fiolhais, C. *Phys. Rev. B* **1992**, *46*, 6671.
(46) Korovina, N. V.; Chang, M. L.; Nguyen, T. T.; Fernandez, R.; Walker, H. J.; Olmstead, M. M.; Gherman, B. F.; Spence, J. D. *Org. Lett.* **2011**, *13*, 3660.
(47) Schreiner, P. R.; Navarro-Vazquez, A.; Prall, M. *Acc. Chem. Res.* **2005**, *38*, 29.
(48) Landquist, J. K. *J. Chem. Soc.* **1953**, 2816.